Considering nonlocality in the optical potentials within eikonal models

C. Hebborn [1,2,*] and F. M. Nunes [3,4,†]

[1] *Facility for Rare Isotope Beams, East Lansing, Michigan 48824, USA*

[2] *Lawrence Livermore National Laboratory, P.O. Box 808, L-414, Livermore, California 94551, USA*

[3] *National Superconducting Cyclotron Laboratory, Michigan State University, East Lansing, Michigan 48824, USA*

[4] *Department of Physics and Astronomy, Michigan State University, East Lansing, Michigan 48824-1321, USA*

(Received 28 May 2021; accepted 14 September 2021; published 24 September 2021)

Background: For its simplicity, the eikonal method is the tool of choice to analyze nuclear reactions at high energies ($E > 100$ MeV/nucleon), including knockout reactions. However, so far, the effective interactions used in this method are assumed to be fully local.

Purpose: Given the recent studies on nonlocal optical potentials, in this work we assess whether nonlocality in the optical potentials is expected to impact reactions at high energies and then explore different avenues for extending the eikonal method to include nonlocal interactions.

Method: We compare angular distributions obtained for nonlocal interactions (using the exact R-matrix approach for elastic scattering and the adiabatic distorted wave approximation for transfer) with those obtained using their local-equivalent interactions.

Results: Our results show that transfer observables are significantly impacted by nonlocality in the high-energy regime. Because knockout reactions are dominated by stripping (transfer to inelastic channels), nonlocality is expected to have a large effect on knockout observables too. Three approaches are explored for extending the eikonal method to nonlocal interactions, including an iterative method and a perturbation theory.

Conclusions: None of the derived extensions of the eikonal model provide a good description of elastic scattering. This paper suggests that nonlocality removes the formal simplicity associated with the eikonal model.

DOI: 10.1103/PhysRevC.104.034624

I. INTRODUCTION

The most versatile probe into the structure of matter in its extreme forms are nuclear reactions. Experimental programs around the world have used a wide variety of reactions to extract a diverse range of information on the properties of different isotopes (e.g., [1–3] for some of the most recent examples). In all these cases, the measured cross sections are interpreted through a reaction model. Regardless of the sophistication level of the reaction model used, the effective interactions between the cluster parts are an essential ingredient to all. These effective interactions are known as optical potentials, because they include an imaginary term, which accounts for all those processes that are not explicitly included in the model.

Even for the simplest case, the effective interaction between a nucleon and a nucleus, optical potentials are intrinsically nonlocal, due to antisymmetrization and coupling to excited modes [4–6]. These features emerge naturally in those potentials derived microscopically from *ab initio* many-body approaches (e.g., [7–10]). Since the early days when Perey and Buck developed their nonlocal optical potential, with a Gaussian nonlocality [11], not many groups have invested in a global nonlocal potential (see [12,13] for recent works on the topic). Most of the phenomenological global optical potentials widely used in the field are approximated to be local for numerical convenience [14–16].

Over the last few years, a large body of work demonstrates that including nonlocality explicitly in the optical potential significantly affects the calculated reactions observables [17–23]. These studies have focused primarily on (d, p) transfer reactions in the energy range $E_{\rm lab} < 50$ MeV. The effects of nonlocality manifest in the short-range part of the bound and scattering wave functions. These effects are then picked up in amplitudes for transfer, evidently dependent on off-shell behavior. In many cases, and particularly for heavier nuclei, the resulting transfer angular distributions calculated with nonlocal optical potentials differ considerably in shape and in magnitude from the local counterparts, and would inevitably lead to discrepancies in the extracted spectroscopic factors.

Given the increasing interest in experiments at higher beam energy using knockout and breakup reactions, it is important to understand the role of nonlocality for energies above 100 MeV/nucleon. These reactions have been extensively used to extract structure information, but their interpretation rely primarily on eikonal methods with local interactions [24–26]. Until now, there have been no investigations on the effects of nonlocality in the optical potential within this energy regime. Neither have the eikonal methods been extended to include the capability of nonlocality in the interactions.

*hebborn@frib.msu.edu

†nunes@nscl.msu.edu

Incorporating nonlocal interactions in the eikonal theory is nontrivial and therefore it is advisable to first inspect whether such extensions would be necessary.

There are two main questions this work is addressing: (1) How large are the effects of nonlocality in the higher energy regime? and (2) what are the challenges in including nonlocality explicitly in the eikonal methods to describe reactions? Since the methods for transfer reactions have already been extended to include nonlocality explicitly, in the first part of this paper we study transfer reactions at energies that are higher than what would normally be used for this type of reaction (>100 MeV/nucleon). Because the stripping mechanism, corresponding to the nonelastic channels where the nucleon is absorbed by the target, is the largest contributor to knockout cross sections [27], if effects turn out to be large for transfer, then effects can also be expected to be large for knockout. Once that is established, we consider a couple of different paths to include nonlocality explicitly in the eikonal formalism.

This paper is organized as follows: In Sec. II we present a brief overview of the two-body local and nonlocal scattering problems. Next, we consider results for transfer reactions (in Sec. III) and elastic scattering (in Sec. IV). In Sec. V we discuss nonlocal extensions of the eikonal model. Conclusions are drawn in Sec. VI.

II. THEORETICAL BACKGROUND

We review in this section the description of the elastic-scattering channel and refer the interested reader to Refs. [28–30] for the calculation of transfer observables.

As usual, we simplify the many-body problem to a two-body one, in which both the projectile P and the target T are assumed structureless and spinless. This reduction comes at a cost, the P-T interaction is simulated through an optical potential, which includes an imaginary part modeling effectively the inelastic channels [4,31].

A. Local interaction

If the P-T interaction is simulated by a local central optical potential V_L, the two-body system is described by the following Schrödinger equation [31]:

$$\left[\frac{P^2}{2\mu} + V_L(\boldsymbol{R})\right]\Psi(\boldsymbol{R}) = E\ \Psi(\boldsymbol{R}), \tag{1}$$

where $\mu = m_P m_T/(m_P + m_T)$ is the P-T reduced mass, $\boldsymbol{P}$ and $\boldsymbol{R} \equiv (\boldsymbol{b}, Z)$ are, respectively, the P-T relative momentum and coordinate and E is the total energy of the system. This equation is solved with the condition that initially the projectile propagates towards the target along the Z axis with a velocity $v = \hbar K/\mu$ and momentum $\hbar K$, i.e.,

$$\Psi(\boldsymbol{R}) \underset{Z\to-\infty}{\longrightarrow} \exp(iKZ). \tag{2}$$

There are several approaches typically used to solve this two-body problem exactly. In this paper, we obtain the exact solution using the R-matrix method combined with the Lagrange-mesh method [32,33]. One of the main advantages of this technique is its straightforward generalization to nonlocal potentials.

The eikonal approximation [24] reflects the fact that at high enough energy the P-T relative motion does not differ much from the initial plane wave. It hence factorizes this plane wave out of the wave function

$$\Psi(\boldsymbol{R}) = \exp(iKZ)\ \widehat{\Psi}(\boldsymbol{R}), \tag{3}$$

and assumes that $\widehat{\Psi}$ varies smoothly with $\boldsymbol{R}$. Furthermore, the eikonal approximation neglects the second derivatives of $\widehat{\Psi}$, simplifying Eq. (1) into [31]

$$i\hbar v\frac{\partial}{\partial z}\widehat{\Psi}(\boldsymbol{b}, Z) = V_L(\boldsymbol{b}, Z)\ \widehat{\Psi}(\boldsymbol{b}, Z), \tag{4}$$

where $\boldsymbol{b}$ is the transverse coordinate of $\boldsymbol{R}$. This simplified Schrödinger equation can be solved analytically and its solutions behave asymptotically as

$$\widehat{\Psi}(\boldsymbol{b}, Z) \underset{Z\to+\infty}{\longrightarrow} \exp\left[-\frac{i}{\hbar v}\int_{-\infty}^{+\infty} V_L(\boldsymbol{b}, Z)\, dZ\right]. \tag{5}$$

In a semiclassical view, the eikonal solutions can be seen as the projectile following a straight-line trajectory at constant impact parameter b and accumulating a phase through its reaction process while interacting with the target.

Elastic-scattering observables depend only on the asymptotic behavior of the wave function, i.e., on the phase in Eq. (5), and are therefore efficiently computed within the eikonal approximation. This model is accurate for reactions at high enough energy [26,34–39]. However, the eikonal description is expected to fail when the wave function differs strongly from a plane wave, i.e., at low energy, small impact parameters and large scattering angles [40–42].

B. Nonlocal interaction

In their most general form, the optical potentials are nonlocal [4]. This nonlocality arises from antisymmetrization of the many-body wave function and the couplings between the different channels. When a nonlocal potential V_{NL} is considered, the Schrödinger equation reads [43]

$$\frac{P^2}{2\mu}\Psi(\boldsymbol{R}) + \int d\boldsymbol{R}'\, V_{NL}(\boldsymbol{R}, \boldsymbol{R}')\Psi(\boldsymbol{R}') = E\ \Psi(\boldsymbol{R}), \tag{6}$$

in which the interaction term is obtained through an integration of the wave function and the nonlocal potential. We solve this equation with the R-matrix method using the same initial condition (2) as in the local case.

In this paper, we first analyze how nonlocality affects transfer (Sec. III) and elastic-scattering (Sec. IV) observables at high energies. Then, we investigate different extensions of the eikonal approximation to the nonlocal Schrödinger equation (6) in Sec. V.

III. EFFECTS OF NONLOCALITY FOR REACTIONS AT HIGH ENERGIES

Although transfer cross sections are not usually measured at high energies due to their low cross sections, it is still interesting to determine the magnitude of the nonlocal effects

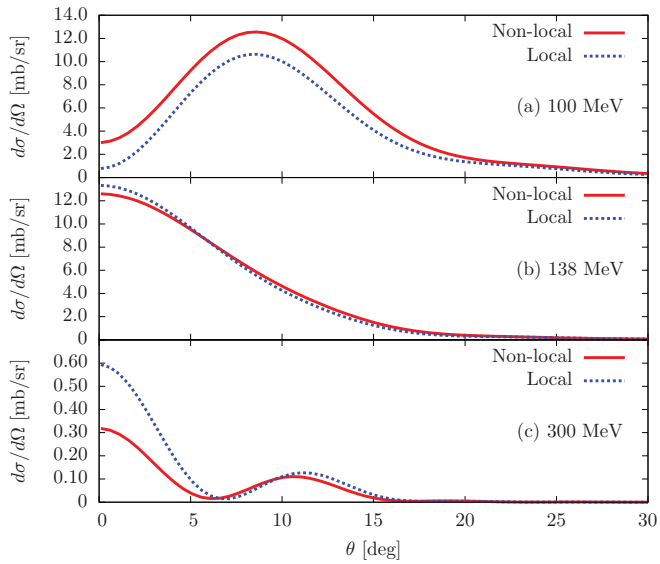

FIG. 1. Comparison of the angular distributions for the ^{208}Pb$(d, p)^{209}$Pb at $E_{\rm lab} = 100$ MeV (top panel), $E_{\rm lab} = 138$ MeV (mid panel) and $E_{\rm lab} = 300$ MeV (bottom panel) obtained with the nonlocal potentials (solid red) and the local-equivalent potentials (dotted blue).

for this channel in this energy regime. Indeed, due to the similarities in the probes, one can expect that if the effects of nonlocality are significant in the transfer channel, they would also be important in stripping, the main contributor to the knockout cross section [27]. The analysis for transfer is possible thanks to the recent generalization of the adiabatic distorted wave approximation (ADWA) formalism [28] including nonlocal interactions [29,30]. This generalization is implemented in the NLAT code, available in Ref. [29].

To evaluate the magnitude of the nonlocal effects at high energies, we take as case study one-neutron transfer reactions ^{208}Pb(d, p) ^{209}Pb at 100 MeV, 138 MeV, and 300 MeV. In the ADWA formalism, the d-^{208}Pb adiabatic potential is built from both n-^{208}Pb and p-^{208}Pb interactions [28], evaluated at half the deuteron energy. In addition, the p-^{209}Pb optical potential in the exit channel is also needed. As in Refs. [17,21], we consider the Perey-Buck nonlocal potentials [11] and we fit with SFRESCO [44] local-equivalent potentials to the nonlocal elastic-scattering observables. The parameters for these interactions can be found in Appendix A. Note that using local-equivalent potentials for the nucleon-target interactions does not guarantee that local and nonlocal adiabatic deuteron potentials are phase-shift equivalent [29,30].

As opposed to [17,21], in this paper we do not consider nonlocality in the bound state wave function. It is well understood that nonlocality in the mean field that binds the neutron in the final state decreases the bound-state wave function in its interior and increases its asymptotic part. Keeping in mind that our aim is to study the effects of nonlocality in eikonal models, and the nonlocal interaction in the bound state calculation is easy to incorporate in these models, here we only focus on the effects of nonlocality in the scattering.

Figure 1 shows the transfer cross sections at 100 MeV (top panel), 138 MeV (mid panel), and 300 MeV (bottom panel) obtained with nonlocal (solid-red lines) and local-equivalent (dotted-blue lines) n-^{208}Pb, p-^{208}Pb, and p-^{209}Pb potentials. At all energies, there is a significant effect of nonlocality at forward angles. At 100 MeV, nonlocality increases the magnitude of the cross section, as already observed in other studies done at lower energy [21], while at larger energies, nonlocality reduces it. Similarly, the integrated cross section increases by 22% at 100 MeV and diminishes by 4% at 138 MeV and 20% at 300 MeV. Surprisingly, nonlocal effects are rather small at 138 MeV compared to the ones observed at 100 MeV and 300 MeV.

Consistent with the analysis of transfer reactions at 50 MeV by Titus *et al.* [21], we find that nonlocality in the deuteron channel has the most influence. Titus *et al.* explain that this is a result of the combination of two effects: the reduction of the amplitude of the deuteron scattering wave function in the interior and an additional phase shift coming from the adiabatic description. Because the present work focuses on reactions at higher energies, where the adiabatic approximation is expected to be more accurate, the deuteron adiabatic local and nonlocal potentials lead to similar phase shifts.

The fact that nonlocality affects the cross section differently at 100 MeV and 300 MeV and does not influence much the transfer observables 138 MeV can be explained by the position of the nodes of the incoming and outgoing scattering wave functions. These nodes cause a compensation of the positive and negative nonlocal contributions to the T matrix and therefore determine if the nonlocality increases or decreases the cross sections at forward angles.

Given the large nonlocal effects on transfer observables at high energies, it is important to also study how nonlocality influences knockout and breakup cross sections in this energy regime. Because eikonal models are the preferred tools to interpret reactions at these energies we must extend the eikonal approximation to include nonlocal interactions.

The development of a nonlocal eikonal model will be presented in Sec. IV. However, because when using an eikonal model the effects of nonlocality on the reaction observable will be mixed with the effects of the eikonal approximation itself, it is crucial to first establish the level of accuracy that can be expected from this approximation at these energies. This is done in the next section.

IV. CONSIDERING APPROXIMATIONS TO ELASTIC SCATTERING

We consider here the elastic scattering of neutrons on ^{208}Pb at 69 MeV and 150 MeV (these energies correspond to half the energy of the cases studied in Sec. III). The n-^{208}Pb interaction is simulated by the same potentials as the ones used in the previous section, which are detailed in Appendix A. For completeness, Fig. 2 shows the scattering wave function resulting from a local (dotted-blue lines) and nonlocal (solid-red lines) interaction. By construction, both potentials lead to identical wave functions at large distances and therefore, for an exact calculation, we expect identical elastic cross sections. What we need to assess is whether this holds under the eikonal approximation.

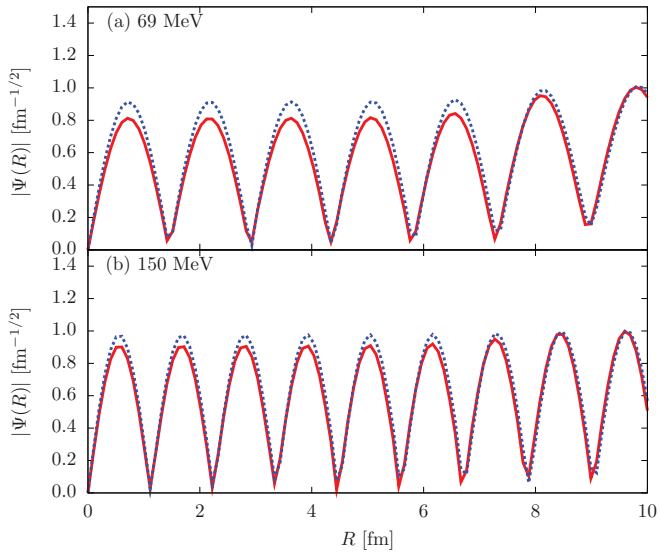

FIG. 2. Scattering wave function for s-wave neutron impinging on ^{208}Pb at 69 MeV (top panel) and 150 MeV (bottom panel), obtained with the nonlocal potentials (solid red) and the local-equivalent potentials (dotted blue).

Figure 3 shows the elastic-scattering cross section as a function of the scattering angle at 69 MeV (top panel) and 150 MeV (bottom panel). The solid-red lines are the exact solutions obtained with the nonlocal potential and the dotted blue lines with the local-equivalent interactions. They agree perfectly with each other except for the largest scattering angles (a limit in the precision of the calculation). Furthermore, the relative difference between the nonlocal and local-equivalent integrated elastic-scattering cross sections calculated using exact methods is less than 3% at 69 MeV and 10% at 150 MeV [45]. As expected, the reduction of the amplitude of the scattering wave function in its interior seen in Fig. 2 does not impact the elastic-scattering cross sections, which only depends on the asymptotic form of these wave functions.

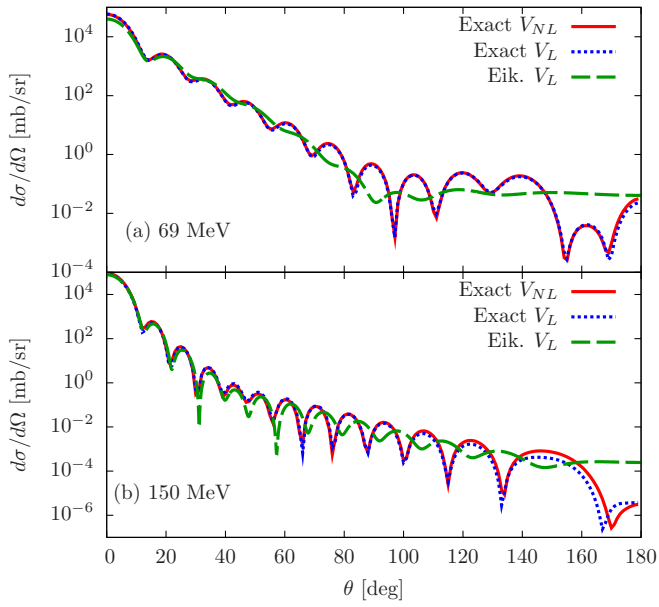

FIG. 3. Elastic-scattering cross section as a function of the scattering angle θ for ^{208}Pb$(n,n)^{208}$Pb at 69 MeV (top panel) and 150 MeV (bottom panel): comparison of the results using the exact nonlocal interaction (red-solid line), the exact local-equivalent (blue-dotted line) and the eikonal local-equivalent (green-dashed line).

We now turn to the calculations using the eikonal approximation (dashed-green lines in Fig. 3). As expected, the eikonal approximation fails to describe the oscillations at large angles at both energies. Surprisingly, it also does not reproduce well the forward angles at 69 MeV, for which it underestimates the exact cross section by 30% at 0°. This discrepancy at forward angles is also visible in integrated elastic-scattering cross sections, which are under-predicted by the eikonal approximation by about 21%. In contrast, at 150 MeV, the eikonal prediction is accurate up to 50° and reproduces roughly the magnitude of the exact distribution in the whole angular range. At this high energy, the relative difference between the exact and eikonal integrated cross sections obtained with the local-equivalent potential is negligible, i.e., about 2%. From this analysis we conclude that the eikonal approximation is valid for the elastic scattering of neutrons around 150 MeV [46].

V. EXPLORING NONLOCAL EXTENSIONS OF THE EIKONAL MODEL

In this section, we study various extensions of the eikonal model to include nonlocal interactions. We consider the same reaction as before, the elastic scattering of neutrons on ^{208}Pb at 69 MeV and 150 MeV.

As detailed in Sec. II, when the interaction is nonlocal, the system is described by the nonlocal Schrödinger equation (6). By reasoning similarly as in the local case and using the same eikonal simplification (3) and (4), Eq. (6) simplifies into

$$i\hbar v \frac{\partial \widehat{\Psi}}{\partial Z}(\boldsymbol{R}) = e^{-iKZ} \int d\boldsymbol{R}'\, V_{NL}(\boldsymbol{R},\boldsymbol{R}')\widehat{\Psi}(\boldsymbol{R}')e^{iKZ'}. \quad (7)$$

This equation has formal solutions, which behave asymptotically as

$$\widehat{\Psi}(\boldsymbol{R}) \underset{Z\to+\infty}{\longrightarrow} -\frac{i}{\hbar v}\int_{-\infty}^{+\infty} dZ \times \int d\boldsymbol{R}'\, V_{NL}(\boldsymbol{R},\boldsymbol{R}')\widehat{\Psi}(\boldsymbol{R}')e^{-iK(Z-Z')}. \quad (8)$$

Following the idea of Titus *et al.* who use an iterative method to include nonlocal interactions in the ADWA [21,29,30], we solve Eq. (7) iteratively and we take as initial wave function, the eikonal solution obtained with the local-equivalent potential.

Figure 4 displays the elastic-scattering cross section at 69 MeV (top panel) and 150 MeV (bottom panel). The exact nonlocal solution corresponds to the solid red lines, the eikonal local-equivalent to the dashed green lines, and the nonlocal eikonal at the first, second, and third iterations to the dash-dotted blue, the dash-dotted-dotted magenta, and the dotted black lines, respectively. At 69 MeV, the first iteration improves slightly the eikonal cross section at 0° by increasing

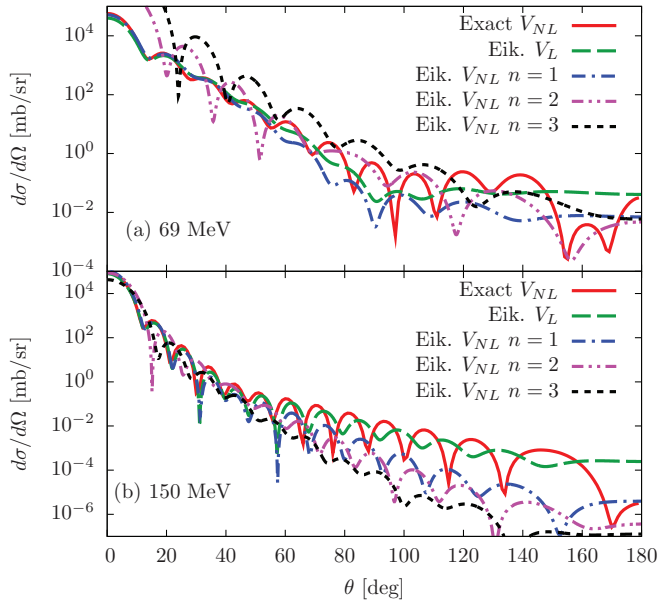

FIG. 4. Elastic-scattering cross section as a function of the scattering angle θ for ^{208}Pb$(n,n)^{208}$Pb at 69 MeV (top panel) and 150 MeV (bottom panel): comparison of the exact nonlocal (solid red), the eikonal local-equivalent (dashed green) and the nonlocal eikonal solutions.

its magnitude, but is less accurate at larger angles. Unfortunately, each additional iteration worsens these results: the cross section is overestimated by several orders of magnitude and the oscillations are not well reproduced. Calculations at 150 MeV, for which the eikonal approximation is more accurate, display a similar behavior, exhibiting a slower divergence with the number of iterations.

This failure of the iterative process can be understood by the fact that the nonlocal potential term [right-hand side of Eq. (7)] integrates the wave function at the previous iteration over the whole radial space. As detailed in Sec. II and illustrated in Sec. IV, the eikonal approximation is valid only for forward angles. In a semiclassical view, this can be interpreted as the eikonal description being accurate at large impact parameters, while it fails at small impact parameters. Since the nonlocal term integrates the eikonal wave function at the previous iteration over the whole radial space, it accumulates errors at each iteration and the accuracy of the corresponding nonlocal eikonal cross sections becomes worst. Naturally, the divergent behavior of the nonlocal eikonal solution is slower at 150 MeV than 69 MeV since the error made by the eikonal approximation is smaller. We have verified that the scattering amplitude is strongly modified at the first iteration at small bs, in the range where the eikonal model describes poorly the wave function. Since the scattering amplitude at the next iteration integrates the wave function at the previous iteration over full space, it is strongly modified at all impact parameters, causing the divergence in the elastic-scattering cross section.

We have investigated two additional implementations of the nonlocal eikonal solution. The first one is also an iterative method but now considering that the potential has nonlocality in the transverse distance b. Although this nonlocality in b is formally easier to handle, ultimately we obtain an expression close to Eq. (7) in which the nonlocal potential term still integrates the wave function at the previous iteration over full space. In this alternative implementation, the wave function also accumulates errors at each iteration and exhibits the same failure as the other iterative process.

Our third implementation is based on a perturbative eikonal solution to the nonlocal problem, detailed in Appendix B. Unfortunately, it too leads to an integral over the full radial range, and eventually diverges with the inclusion of higher orders.

We note that all nonlocal extensions of the eikonal approximation considered in this paper fail for essentially the same reason: The nonlocal correction is strongly dependent on the short-range description of the scattering wave function, which is not well described by the eikonal approximation. This leads to our conclusion that in the framework we considered, the eikonal method is not suitable to handle nonlocal interactions. Only methods that are able to provide accurate scattering wave functions over the whole radial range can be a useful starting point for extensions to nonlocal optical potentials based on an iterative approach.

VI. CONCLUSIONS

Even though in their most general form, optical potentials are nonlocal, many reaction models have not been adapted to deal with this nonlocality. It has been shown that nonlocality affects strongly transfer observables [17–23]. Since these studies were limited to low energy, in this paper we investigated the importance of these effects in the higher energy regime, the regime for which knockout reactions are typically measured. We extended the study of Ref. [21] to these energies, i.e., above 50 MeV/nucleon, and analyze the nonlocal effects in the projectile-target potentials for (d,p) transfer reactions. Our results show that nonlocality affects strongly transfer angular distributions and therefore are likely to influence significantly the stripping process, which is the largest contributor to knockout observables.

Because knockout reactions are usually analyzed with eikonal models, we then investigated the extension of this theory to include nonlocal interactions. We considered elastic scattering of neutrons on a ^{208}Pb target. Following the same idea used in Ref. [29,30], we adopted an iterative method to obtain the solution of the nonlocal scattering equation, in which the nonlocal correction involves a radial integration of the product of eikonal wave function at the previous iteration and the nonlocal potential. Our results show that this iterative solution diverges because the eikonal solution is not accurate at short distances, causing an accumulation of errors at each iteration. Other approaches were considered but turned out to suffer from the same problem.

This analysis suggests that models that provide an accurate description of the wave function over its whole radial range are better suited to describe high-energy reactions such as knockout and breakup, when incorporating nonlocal interactions iteratively. This includes the distorted wave Born approximation, the continuum-discretized coupled channel method [47,48] or the dynamical eikonal approximation [36].

ACKNOWLEDGMENTS

The authors would like to thank P. Capel for useful discussions. The work of C.H. is supported by the U.S. Department of Energy, Office of Science, Office of Nuclear Physics, under the FRIB Theory Alliance Award No. DE-SC0013617 and under Work Proposal No. SCW0498. This work was prepared in part by LLNL under Contract No. DE-AC52-07NA27344. This work was supported by the National Science Foundation under Grant No. PHY-1811815 and the U.S. Department of Energy Grant No. DE-SC0021422. This work relied on iCER and the High Performance Computing Center at Michigan State University for computational resources.

APPENDIX A: CHOICE OF POTENTIALS

In this paper, we study one-neutron transfer reactions ^{208}Pb$(d, p)^{209}$Pb at 100 MeV, 138 MeV and 300 MeV. To model these reactions within the ADWA, we use single-particle local potentials to generate the bound states, and optical potentials to simulate the projectile-target interactions in the entrance and exit channels.

As in Ref. [29], the deuteron bound state is produced by a Gaussian potential of range 1.494 fm and a depth of 71.85 MeV. We also adopt the same description of ^{209}Pb as in Ref. [29], using a real single-particle ^{208}Pb-n potential composed of a volume and a spin-orbit term. The central Woods-Saxon shape is characterized by a radius of 7.406 fm and a diffuseness of 0.65 fm. The depths are fitted to reproduce the valence neutron binding energy of ^{209}Pb, the real depth is given by 46.561 MeV and the spin-orbit strength by 6 MeV.

The optical potentials needed for the ADWA reaction model are $V(n\text{-}^{208}\text{Pb})$, $V(p\text{-}^{208}\text{Pb})$ at half the deuteron incident energy and $V(p\text{-}^{209}\text{Pb})$ at the energy in the exit channel. We take the nonlocal interaction developed by Perey and Buck [11] defined by

$$V_{NL}(\boldsymbol{R}, \boldsymbol{R}') = V(\tilde{R}) \frac{\exp\left[-\left(\frac{|\boldsymbol{R}-\boldsymbol{R}'|}{\beta}\right)^2\right]}{\pi^{3/2}\beta^3}, \tag{A1}$$

with $\tilde{R} = (R + R')/2$. The local part of this potential is parametrized with a Woods-Saxon form as

$$V(R) = -V_R\, f_{\rm WS}(R, R_R, a_R) - i\, W_I\, f_{\rm WS}(R, R_I, a_I) + i\, 4 a_D W_D \frac{d}{dR} f_{\rm WS}(R, R_D, a_D), \tag{A2}$$

where

$$f_{\rm WS}(R, R_X, a_X) = \frac{1}{1 + e^{\frac{R-R_X}{a_X}}}. \tag{A3}$$

The parameters of the Perey-Buck interactions are given in Table I [50]. This potential is energy-independent, therefore the same parameters are used for all energies considered.

For a meaningful comparison, we build the local-equivalent potentials V_L by fitting with SFRESCO [44] the exact elastic-scattering observables obtained from the nonlocal interactions and with an artificial relative error of 10%. These potentials are parametrized with a Woods-Saxon form (A2) and (A3) and the corresponding parameters are displayed in Table I. In the last column, we present the χ^2/N resulting from each fit.

Of course, the Coulomb interaction is local and we take it to be that of a uniformly charged sphere of radius $R_C = 1.25 \times A_T^{1/3}$ fm, with A_T the mass number of the target.

APPENDIX B: PERTURBATIVE NONLOCAL EIKONAL SOLUTIONS

In this Appendix, we study an alternative eikonal solution to the nonlocal Schrödinger equation (6). Following a perturbative approach, we write the nonlocal potential as a sum of a local and nonlocal terms, i.e, $V_{NL}(\boldsymbol{R}, \boldsymbol{R}') = V_L(R) + \Delta V_{NL}(\boldsymbol{R}, \boldsymbol{R}')$, and treat ΔV_{NL} as a perturbation. We take for V_L the local-equivalent potential and for $\Delta V_{NL} = V_{NL} - V_L$ the difference between the nonlocal potential and the local-equivalent one.

Accordingly, the eikonal wave functions can be expressed as the sum of a leading term $\widehat{\Psi}^0$ and a perturbation $\widehat{\Psi}^1$

$$\widehat{\Psi}(\boldsymbol{R}) = \widehat{\Psi}^0(\boldsymbol{R}) + \widehat{\Psi}^1(\boldsymbol{R}). \tag{B1}$$

TABLE I. Parameters of the potentials: the nonlocal interactions are taken from Ref. [11] and their local-equivalent are fitted with SFRESCO [44].

			V_R (MeV)	R_R (fm)	a_R (fm)	W_I (MeV)	R_I (fm)	a_I (fm)	W_D (MeV)	R_D (fm)	a_D (fm)	β (fm)	χ^2/N
	n-^{208}Pb		71	7.229	0.650				15	7.229	0.470	0.85	
V_{NL}	p-^{208}Pb												
	p-^{209}Pb		71	7.240	0.650				15	7.240	0.470	0.85	
		50 MeV	34.153	7.435	0.610				8.174	7.314	0.422		$\chi^2/N = 0.229$
	n-^{208}Pb	69 MeV	29.475	7.416	0.621	0.280	8.876	0.400	6.711	7.318	0.400		$\chi^2/N = 2.237$
		150 MeV	15.783	7.355	0.580				4.005	7.284	0.406		$\chi^2/N = 6.600$
V_L		50 MeV	38.969	7.434	0.615				9.030	7.324	0.420		$\chi^2/N = 0.261$
	p-^{208}Pb	69 MeV	33.755	7.424	0.606				7.818	7.332	0.415		$\chi^2/N = 1.282$
		150 MeV	20.303	7.244	0.639				4.672	7.274	0.401		$\chi^2/N = 4.234$
		101.7 MeV	26.092	7.412	0.612				5.867	7.339	0.398		$\chi^2/N = 2.401$
	p-^{209}Pb	139.7 MeV	17.790	7.426	0.596				3.857	7.355	0.369		$\chi^2/N = 0.895$
		301.7 MeV	6.151	7.029	0.614				1.434	7.276	0.400		$\chi^2/N = 3.365$

In the eikonal approximation, the leading term $\widehat{\Psi}^0$ is simply the local-equivalent eikonal solution (5). The first-order term is obtained from the nonlocal eikonal equation

$$i\hbar v\frac{\partial\widehat{\Psi}^1}{\partial Z}(\boldsymbol{R}) = V_L(R)\widehat{\Psi}^1(\boldsymbol{R}) + e^{-iKZ}\int d\boldsymbol{R}'\,\Delta V_{NL}(\boldsymbol{R},\boldsymbol{R}')e^{iKZ'}\widehat{\Psi}^0(\boldsymbol{R}'). \tag{B2}$$

Note that the nonlocal term of this equation depends on the eikonal solution $\widehat{\Psi}^0$, similarly as in the iterative method explored in Sec. IV. The nonlocal eikonal perturbative equation (B2) can be solved analytically, its solutions tend to

$$\widehat{\Psi}^1(\boldsymbol{R}) \underset{Z\to+\infty}{\longrightarrow} -\frac{i}{\hbar v}e^{-\frac{i}{\hbar v}\int_{-\infty}^{+\infty}dZ\,V_L(R)} \times\int_{-\infty}^{+\infty}dZ\,e^{-iKZ}e^{\frac{i}{\hbar v}\int_{-\infty}^{Z}dZ'\,V_L(R')} \times\int d\boldsymbol{R}'\,\Delta V_{NL}(\boldsymbol{R},\boldsymbol{R}')e^{iKZ'}\widehat{\Psi}^0(\boldsymbol{R}'). \tag{B3}$$

Figure 5 shows the elastic-scattering cross section for neutron scattering on ^{208}Pb target at 69 MeV (top panel) and 300 MeV (bottom panel), as a function of the scattering angle. The leading-order eikonal perturbative solution (dashed green lines) is simply the local-equivalent eikonal cross section. As already noted in Sec. IV, it reproduces well the magnitude of the exact nonlocal cross sections (solid-red lines) at 0° at 300 MeV energies but not at 69 MeV. Also, it is not accurate at larger angles, mostly due to the eikonal approximation, which is inadequate at the largest angles.

The cross sections obtained with the first-order perturbation of the nonlocal eikonal solution (A3) are plotted by the dash-dotted-dotted orange lines. At both energies, the first-order calculation worsens the result. Even when considering a different leading order solution, viz., by using the local diagonal part of the nonlocal potential for V_L, we arrive at the same issue. Just as in the analysis of the iterative solution in Sec. IV, this failure can be explained by the inaccuracy of the eikonal wave function at short distances, which leads to large errors in the integral associated with the nonlocal correction. Unfortunately, this perturbative approach also fails to extend the eikonal method to include nonlocal interactions.

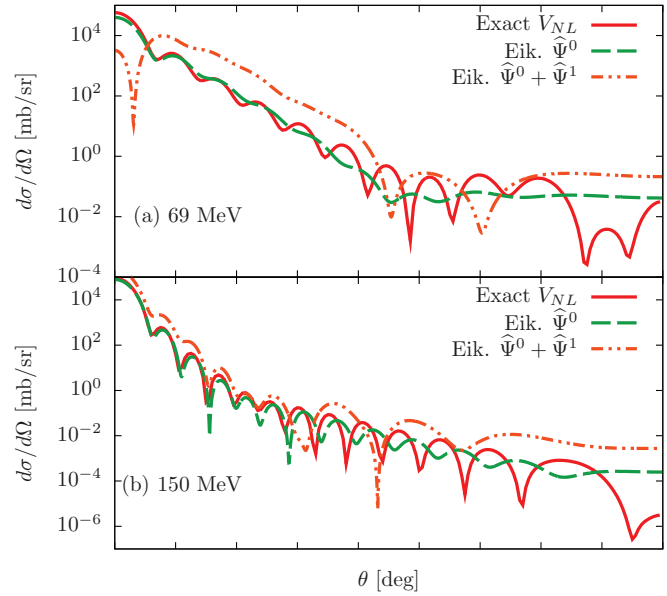

FIG. 5. Elastic-scattering cross section as a function of the scattering angle θ for ^{208}Pb$(n,n)^{208}$Pb at 69 MeV (top panel) and 150 MeV (bottom panel): comparison of the exact nonlocal (solid red) and the perturbative eikonal solutions.

[1] Z. H. Yang, Y. Kubota, A. Corsi, K. Yoshida, X.-X. Sun, J. G. Li, M. Kimura, N. Michel, K. Ogata, C. X. Yuan, Q. Yuan, G. Authelet, H. Baba, C. Caesar, D. Calvet, A. Delbart, M. Dozono, J. Feng, F. Flavigny, J.-M. Gheller *et al.*, Phys. Rev. Lett. **126**, 082501 (2021).

[2] K. Wang, Y. Y. Yang, A. M. Moro, V. Guimaraes, J. Lei, D. Y. Pang, F. F. Duan, J. L. Lou, J. C. Zamora, J. S. Wang, Z. Y. Sun, H. J. Ong, X. Liu, S. W. Xu, J. B. Ma, P. Ma, Z. Bai, Q. Hu, X. X. Xu *et al.*, Phys. Rev. C **103**, 024606 (2021).

[3] B. P. Kay, J. P. Schiffer, S. J. Freeman, T. L. Tang, B. D. Cropper, T. Faestermann, R. Hertenberger, J. M. Keatings, P. T. MacGregor, J. F. Smith, and H. F. Wirth, Phys. Rev. C **103**, 024319 (2021).

[4] H. Feshbach, Ann. Phys. (NY) **5**, 357 (1958).

[5] L. Canton, G. Pisent, J. P. Svenne, D. van der Knijff, K. Amos, and S. Karataglidis, Phys. Rev. Lett. **94**, 122503 (2005).

[6] P. Fraser, K. Amos, S. Karataglidis, L. Canton, G. Pisent, and J. Svenne, Euro. Phys. J. A **35**, 69 (2008).

[7] J. Rotureau, P. Danielewicz, G. Hagen, F. M. Nunes, and T. Papenbrock, Phys. Rev. C **95**, 024315 (2017).

[8] J. Rotureau, P. Danielewicz, G. Hagen, G. R. Jansen, and F. M. Nunes, Phys. Rev. C **98**, 044625 (2018).

[9] A. Idini, C. Barbieri, and P. Navrátil, Phys. Rev. Lett. **123**, 092501 (2019).

[10] T. R. Whitehead, Y. Lim, and J. W. Holt, arXiv:2009.08436.

[11] F. Perey and B. Buck, Nucl. Phys. **32**, 353 (1962).

[12] Y. Tian, D.-Y. Pang, and Z.-Y. Ma, Int. J. Mod. Phys. E **24**, 1550006 (2015).

[13] A. E. Lovell, P.-L. Bacq, P. Capel, F. M. Nunes, and L. J. Titus, Phys. Rev. C **96**, 051601(R) (2017).

[14] A. Koning and J. Delaroche, Nucl. Phys. **A713**, 231 (2003).

[15] R. Varner, W. Thompson, T. McAbee, E. Ludwig, and T. Clegg, Phys. Rep. **201**, 57 (1991).

[16] F. D. Becchetti, Jr. and G. W. Greenlees, Phys. Rev. **182**, 1190 (1969).

[17] L. J. Titus and F. M. Nunes, Phys. Rev. C **89**, 034609 (2014).

[18] A. Ross, L. J. Titus, F. M. Nunes, M. H. Mahzoon, W. H. Dickhoff, and R. J. Charity, Phys. Rev. C **92**, 044607 (2015).

[19] N. K. Timofeyuk and R. C. Johnson, Phys. Rev. Lett. **110**, 112501 (2013).

[20] S. J. Waldecker and N. K. Timofeyuk, Phys. Rev. C **94**, 034609 (2016).
[21] L. J. Titus, F. M. Nunes, and G. Potel, Phys. Rev. C **93**, 014604 (2016).
[22] A. Ross, L. J. Titus, and F. M. Nunes, Phys. Rev. C **94**, 014607 (2016).
[23] W. Li, G. Potel, and F. Nunes, Phys. Rev. C **98**, 044621 (2018).
[24] R. J. Glauber, in *Lectures in Theoretical Physics*, edited by W. E. Brittin and L. G. Dunham (Interscience, New York, 1959), Vol. 1, p. 315.
[25] M. S. Hussein and K. W. McVoy, Nucl. Phys. A **445**, 124 (1985).
[26] P. G. Hansen and J. A. Tostevin, Ann. Rev. Nucl. Part. Sc. **53**, 219 (2003).
[27] J. Lei and A. Bonaccorso, Phys. Lett. B **813**, 136032 (2021).
[28] R. C. Johnson and P. C. Tandy, Nucl. Phys. A **235**, 56 (1974).
[29] L. Titus, A. Ross, and F. Nunes, Comput. Phys. Commun. **207**, 499 (2016).
[30] L. J. Titus, Ph.D. thesis, Michigan State University, 2016.
[31] D. Baye and P. Capel, in *Clusters in Nuclei, Vol. 2*, edited by C. Beck, Lectures Notes in Physics Vol. 848 (Springer, Heidelberg, 2012), p.121.
[32] P. Descouvemont and D. Baye, Rep. Prog. Phys. **73**, 036301 (2010).
[33] D. Baye, Phys. Rep. **565**, 1 (2015).
[34] K. Ogata, M. Yahiro, Y. Iseri, T. Matsumoto, and M. Kamimura, Phys. Rev. C **68**, 064609 (2003).
[35] C. A. Bertulani, Phys. Rev. Lett. **94**, 072701 (2005).
[36] D. Baye, P. Capel, and G. Goldstein, Phys. Rev. Lett. **95**, 082502 (2005).
[37] K. Ogata and C. A. Bertulani, Prog. Theor. Phys. **123**, 701 (2010).
[38] E. C. Pinilla, P. Descouvemont, and D. Baye, Phys. Rev. C **85**, 054610 (2012).
[39] L. Moschini and P. Capel, Phys. Lett. B **790**, 367 (2019).
[40] J. S. Al-Khalili, J. A. Tostevin, and J. M. Brooke, Phys. Rev. C **55**, R1018 (1997).
[41] C. Hebborn and P. Capel, Phys. Rev. C **96**, 054607 (2017).
[42] C. Hebborn and P. Capel, Phys. Rev. C **98**, 044610 (2018).
[43] N. Austern, Phys. Rev. **137**, B752 (1965).
[44] I. J. Thompson, Comput. Phys. Rept. **7**, 167 (1988).
[45] For the local-equivalent potential at 150 MeV, we have also considered the prescription by Perey and Buck given in Eq. (35) of Ref. [11]. It reproduces the non-local cross sections at forward angles but is less accurate than the local-equivalent potential fitted by SFRESCO at larger angles. The corresponding integrated cross section underestimates the non-local one by 17%.
[46] We should note that for charged particle collisions the situation is different. Then the forward-angles scattering is dominated by the Coulomb interaction, which is typically treated exactly for two-body collisions within the eikonal approximation [49]. In such a case the eikonal model would lead to accurate cross sections for the elastic scattering of charged nuclei, even at energies as low as 50 MeV/nucleon [40–42].
[47] M. Kamimura, M. Yahiro, Y. Iseri, H. Kameyama, Y. Sakuragi, and M. Kawai, Prog. Theor. Phys. Suppl. **89**, 1 (1986).
[48] M. Yahiro, K. Ogata, T. Matsumoto, and K. Minomo, Prog. Theor. Exp. Phys. **2012**, 01A206 (2012).
[49] C. A. Bertulani and P. Danielewicz, *Introduction to Nuclear Reactions* (Institute of Physics Publishing, Bristol, 2004).
[50] We neglect the spin-orbit term for simplicity.